

# Randomized OFDM for Multi-cell Environments<sup>1</sup>

LI PING

Department of EE, City University of Hong Kong, Tat Chee Avenue, Kowloon Hong Kong  
*email: eeliping@cityu.edu.hk*

**Abstract:** This paper is concerned with a randomized OFDM (R-OFDM) scheme. The basic principle is to apply a scrambling operation to several OFDM frames. With a proper design strategy, the scrambling operation will not affect intra-cell orthogonality of OFDM (even considering multi-path effect). For signals from different cells, mutually random scramblings are used to reduce their correlation. This alleviates the worst case inter-cell interference problem. R-OFDM combines some advantages of both OFDM and CDMA, namely, intra-cell interference avoidance, cross-cell interference mitigation as well as simple receiver structure.

## 1 INTRODUCTION

OFDM (Orthogonal Frequency Division Multiplexing) is a promising technique for high data rate transmission over dispersive channels [1,2]. It has been successfully selected as modulation schemes in the European Audio Broadcasting standard and indoor standards such as ETSI-Hiperlan-II and IEEE 802.11. OFDM and related schemes have also been considered for many other applications [3-10].

If carriers are re-used in a multi-cell system, multiple access interference (MAI) becomes a serious problem due to the correlation problem. Worst-case MAI is particularly damaging between two signals occupying the same carrier. It imposes a limit on system performance and capacity. This is a major problem for the use of OFDM technique in cellular systems.

This paper is concerned with a randomized OFDM (R-OFDM)<sup>2</sup> scheme with potential CDMA-type one-cell spectrum re-use deployment (i.e., one spectrum re-used for all the cells). Further to the basic principle introduced in [11], this paper provides a detailed study on issues of interference characteristics, clipping effect and low-cost transceiver design.

The followings are some main features of R-OFDM.

- Convolutional scrambling and de-scrambling operations are used at the transmitter and receiver respectively, which are commutative with the multi-

path effect (through the prefix technique), so the properties discussed below can be maintained in multi-path channels.

- For same-cell-users, the scrambling and de-scrambling operations cancel each other. They do not affect the orthogonality among the sequences used within a cell so the system behaves just like normal OFDM.
- Mutually (approximately) random scrambling schemes are applied to signals in neighboring cells. They result in Gaussian-noise-like cross-cell interference behavior. It has a more benign effect than the interference resulted from fully correlated signals.

The randomization operation introduces a CDMA ingredient into R-OFDM and alleviates the worst case cross-cell MAI problem. R-OFDM combines some advantages of both OFDM and CDMA, namely, intra-cell interference avoidance, cross-cell interference mitigation as well as simple receiver structure. It can potentially achieve higher spectrum efficiency compared with either the standard OFDM or CDMA in cellular environments. As a particular scheme of intra-cell interference suppression, R-OFDM has the advantage of considerably lower receiver complexity compared with other multi-user detection schemes [12].<sup>3</sup>

---

<sup>1</sup>This work was supported by a City University of Hong Kong Strategic Research Grant (No. 7000804).

<sup>2</sup>The system model was originally called OFDM-CsDMA in [11] that is somehow confusing. The term R-OFDM used here is simpler and more appropriate.

---

<sup>3</sup>Theoretically, a CDMA receiver based on multi-user detection is able to suppress any interference, but intra-cell interference cancellation (treating other-cell interference as Gaussian noise) is most feasible due to complexity concerns. This results in similar principle as that discussed in this paper.

Compared with other existing work, orthogonal separation of up-link users is still an issue for combined OFDM-CDMA schemes. Due to alignment error and independent fading experienced by signals from different users, it is difficult to apply some existing OFDM-CDMA [4,5,7,8] detection methods in the up-link. There is an interesting recent work on up-link multiple access [9]. It is demonstrated in [9] that by allowing certain tolerance on the alignment error of OFDM frames, the overhead in handling the up-link synchronization problem can be significantly reduced. The work in [9] is for a single cell environment. Incorporating R-OFDM with the scheme in [9] can be an interesting future work.

When used for the up-link, approximate frame alignment among same-cell users is assumed in R-OFDM. The prefix technique for treating multi-path delay can also be used to treat the frame alignment errors (since they have the same effect seen from a receiver). Due to the overhead involved, R-OFDM is most suitable for low speed, small cell-size systems (such as indoor systems) where synchronization accuracy is not a difficult issue.

## 2 PRELIMINARIES

### 2.1 CYCLIC CONVOLUTIONS, DFT, IDFT AND ORTHOGONAL PHASOR SEQUENCES

Let  $\mathbf{x}=\{x_n\}$  and  $\mathbf{y}=\{y_n\}$  be two length- $N$  discrete sequences and  $\langle n-n' \rangle \equiv n-n'$  modulo  $N$ . The cyclic convolution between  $\mathbf{x}$  and  $\mathbf{y}$ , denoted as  $\mathbf{z}=\mathbf{x} \circledast \mathbf{y}$ , is defined by

$$z_n = \sum_{n'=0}^{N-1} x_{n'} y_{\langle n-n' \rangle} \quad 0 \leq n \leq N-1 \quad (1)$$

The multi-path effect in a digital communication system is usually modeled by a sliding convolution but it can be transformed into a cyclic one with a prefix technique, see [11].

The  $N$ -point unitary *DFT* (Discrete Fourier Transform) of a sequence  $\mathbf{x}$  and its inverse *IDFT* (Inverse *DFT*) are listed below [13],

$$DFT: \quad \mathbf{X} = \{X_k\} = F(\mathbf{x}) = \left\{ \frac{1}{\sqrt{N}} \sum_{i=0}^{N-1} x_i e^{-\frac{j2\pi ik}{N}} \right\} \quad (2a)$$

$$IDFT: \quad \mathbf{x} = \{x_i\} = F^{-1}(\mathbf{X}) = \left\{ \frac{1}{\sqrt{N}} \sum_{k=0}^{N-1} X_k e^{\frac{j2\pi ik}{N}} \right\} \quad (2b)$$

Define an orthogonal sequence set,

$$\mathbf{x}^{(k)} \triangleq \left\{ \frac{1}{\sqrt{N}}, \frac{1}{\sqrt{N}} e^{\frac{j2\pi p \times k}{N}}, \dots, \frac{1}{\sqrt{N}} e^{\frac{j2\pi p \times (N-1)k}{N}} \right\}$$

$$k = 0, 1, \dots, N-1 \quad (3)$$

*DFT* and *IDFT* can also be redefined in the vector form as

$$DFT: \quad F(\mathbf{x}) = \sum_{i=0}^{N-1} x_i \bar{\mathbf{x}}^{(i)} \quad (4a)$$

$$IDFT: \quad F^{-1}(\mathbf{X}) = \sum_{k=0}^{N-1} X_k \mathbf{x}^{(k)} \quad (4b)$$

where  $\bar{\mathbf{x}}^{(k)}$  is the conjugate of  $\mathbf{x}^{(k)}$ . The following is a well-known relationship [13],

$$F[\mathbf{x} \circledast \mathbf{y}] = \sqrt{N} \mathbf{X} \circ \mathbf{Y} = \sqrt{N} \{X_k Y_k\} \quad (5)$$

where “ $\circ$ ” denotes the symbol-by-symbol product of two sets.

### 2.2 OFDM TRANSMISSION PRINCIPLES

The OFDM transmission principle [1] is illustrated in figure 1. The input is delivered in a framed structure. An *IDFT* is applied to each input frame so that  $\mathbf{v}=F^{-1}(\mathbf{u})$ . The resultant signal is transmitted using quadrature amplitude modulation (QAM). The cyclic prefix technique [1,11] is applied at this point. It is well-known [1,11] that the following end-to-end transmission model results from the use of prefixes,

$$\hat{\mathbf{v}} = \mathbf{v} \circledast \mathbf{c} + \mathbf{h} \quad (6)$$

where  $\mathbf{c}$  is a sequence of reflection coefficients and  $\mathbf{h}$  a sequence of additive noise. Applying a *DFT* to  $\hat{\mathbf{v}}$  in (6) and using (5), we have (recall that  $\mathbf{v}=F^{-1}(\mathbf{u})$ )

$$\hat{\mathbf{u}} = F(\hat{\mathbf{v}}) = \sqrt{N} \mathbf{u} \circ F(\mathbf{c}) + F(\mathbf{h}) \quad (7a)$$

or in a symbol-by-symbol form,

$$\hat{u}_k = \sqrt{N} u_k C_k + \mathbf{H}_k \quad k = 0, 1, \dots, N-1 \quad (7b)$$

where  $\{C_k\}=F(\mathbf{c})$  and  $\{\mathbf{H}_k\}=F(\mathbf{h})$ . Equation (7b) implies an orthogonal property, i.e., there is no cross interference among carriers for different  $u_k$ . Clearly,  $\hat{u}_k$  can be used to estimate  $u_k$  provided that the fading factor  $C_k$  is known.

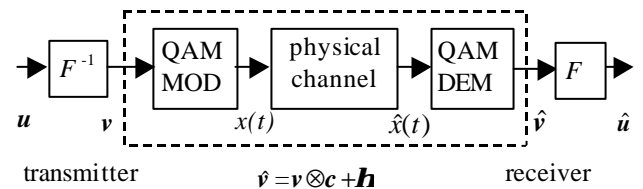


Figure 1. The OFDM transmission principle. Sequence  $\mathbf{v}$  is padded with a cyclic prefix before transmission, which is stripped off at the receiver.

### 2.3 OFDM CARRIERS AND FREQUENCIES

From (4), the transmitter and receiver functions for OFDM can be alternatively expressed as

$$\mathbf{v} = \sum_k u_k \mathbf{x}^{(k)} \quad (8a)$$

$$\hat{u}_k = \langle \hat{\mathbf{v}}, \overline{\mathbf{x}}^{(k)} \rangle \quad (8b)$$

Equations (8a) and (8b) are convenient for interference analysis (but realization based on figure 1 using FFT is more efficient). We will refer to  $\mathbf{x}^{(k)}$  as an OFDM carrier of frequency index  $k$ . Prefix can be represented by extending  $\mathbf{x}^{(k)}$  appropriately in (8a).

### 3 R-OFDM: INTRA-CELL TRANSMISSION PRINCIPLES

In principle, a standard OFDM system can re-use the same set of orthogonal carriers  $\{\mathbf{x}^{(k)}\}$  in a multi-cell environment, but the correlation among the re-used carriers is a serious interference problem. The worst-case MAI (such as the wanted and interfering signals occupying the same OFDM carrier) is a limiting factor in this case. The situation is similar to ordinary FDMA with frequency re-use.

In the following, we will investigate a randomization technique to alleviate the cross-cell interference problem in OFDM system. The basic strategy is to introduce a pair of scrambling/de-scrambling operations at the transmitter and receiver respectively. Different scrambling/de-scrambling pairs are assigned to different cells. For users in the same cell, the two operations cancel each other. An important property of this approach is that the intra-cell orthogonality can be maintained in a multi-path channel, as shown below.

#### 3.1 SYSTEM MODEL

The R-OFDM transmission principle is shown in figure 2. Compared with the standard OFDM in figure 1(b), the difference is the convolutions involving  $\mathbf{p}$ . We impose a constraint on  $\mathbf{p}$ ,

$$\mathbf{p} \otimes \mathbf{p} = \mathbf{d} = \{1, 0, 0, \dots, 0\} \quad (9)$$

Here for simplicity, we assume that  $\mathbf{p}$  is real (For complex  $\mathbf{p}$ , (9) can be modified to  $\mathbf{p} \otimes \mathbf{p}^* = \mathbf{d}$ ). The construction of  $\mathbf{p}$  is discussed in section 5 and the Appendix. According to (5) and (9),

$$F(\mathbf{p}) \circ F(\mathbf{p}) = F(\mathbf{p} \otimes \mathbf{p}) / \sqrt{N} = F(\mathbf{d}) / \sqrt{N} = \{1/N, \dots, 1/N\}$$

We then have the following property for  $\mathbf{p}$ .

**Remark 1:** The DFT of  $\mathbf{p}$  is a binary sequence of  $\pm 1/\sqrt{N}$ .

For simplicity we ignore channel noise and concentrate on multi-path effect. (It can be shown that the same principle applies considering channel noise, see [11].) In figure 2, every length- $N$   $\mathbf{v}$ -frame contains  $L$  sub-frames together with their prefixes. Each sub-frame is the IDFT of  $M$  input symbols, with  $M < N$ . If a user delivers less than  $M$  symbols per  $\mathbf{u}$ -frame, then  $\mathbf{u}$  can be filled with an appropriate number of zeros. In particular, a  $\mathbf{u}$ -frame can contain only one non-zero symbol and after IDFT there is only one active non-zero carrier. This scheme will be detailed in 3.3.

In figure 2,  $L$  sub-frames are convoluted together with  $\mathbf{p}$  for good randomization effect (see Section 4). An extra cyclic prefix is padded to the transmitted sequence  $\mathbf{w}$  to convert the multi-path effect into a cyclic convolution  $\hat{\mathbf{w}} = \mathbf{c} \otimes \mathbf{w}$ . Then, due to the commutative property of convolutions and (9),

$$\hat{\mathbf{v}} = \mathbf{v} \otimes \mathbf{p} \otimes \mathbf{c} \otimes \mathbf{p} = \mathbf{v} \otimes \mathbf{c} \otimes \mathbf{d} = \mathbf{v} \otimes \mathbf{c} \quad (10)$$

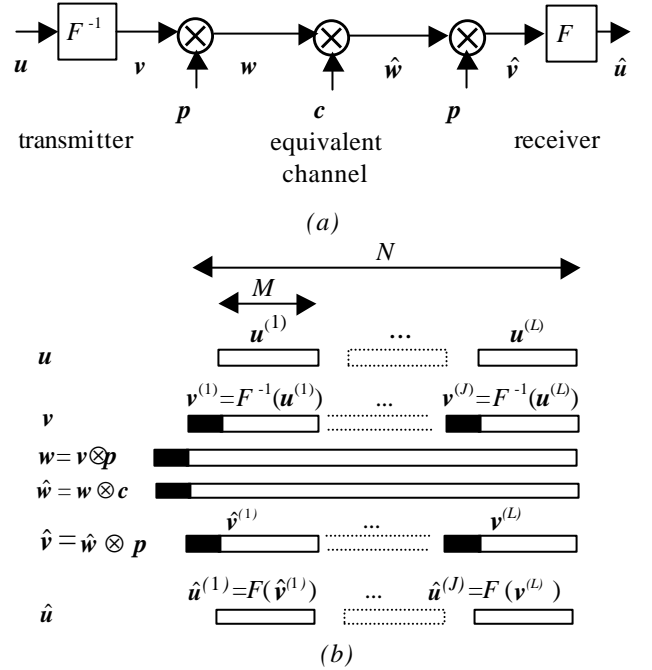


Figure 2. (a) Overview of R-OFDM transmission between a pair of designated users. Channel noise is ignored. Due to the commutative property and (9), the two convolutions shown cancel each other. (b) Signal structure of R-OFDM. The black signals represent prefixes. Notice that  $\mathbf{v}$  consists of  $L$  sub-frames, each individually generated from the IDFT of  $M$  input symbols and padded with a prefix. An extra prefix is padded to  $\mathbf{w}$  before transmission to ensure  $\hat{\mathbf{w}} = \mathbf{w} \otimes \mathbf{c}$ . The prefixes are successively stripped off at the receiver.

Equation (10) indicates that the two convolutions in figure 2(a) cancel each other. In other words, they are transparent to *IDFT* and *DFT* at the two ends. As shown in figure 2(b), every sub-frame  $\mathbf{v}^{(j)}$  in  $\mathbf{v}$  is padded with a cyclic prefix. After stripping off the prefixes at the receiver, we have,

$$\hat{\mathbf{v}}^{(j)} = \mathbf{v}^{(j)} \otimes \mathbf{c} \quad (11a)$$

With the *DFT* operation, we again have

$$\hat{\mathbf{u}}^{(j)} = \sqrt{N} \mathbf{u}^{(j)} \circ F(\mathbf{c}) \quad (11b)$$

Comparing this with (7) and ignoring the additive noise, it is seen that the systems in figures 1 and 2 are equivalent, provided that the transmitter and receiver are based on the same  $\mathbf{p}$ .

### 3.2 A DFT DOMAIN VIEW

A *DFT* domain view can provide more insight. From Remark 1, the convolution  $\mathbf{w} = \mathbf{v} \otimes \mathbf{p}$  at the transmitter only introduces a sign change in the *DFT* spectrum of  $\mathbf{v}$  without affecting its power spectrum. Thus we can regard  $\mathbf{w} = \mathbf{v} \otimes \mathbf{p}$  as introducing a binary phase randomization. At the receiver end, another matching sign change, realized by the second convolution with the same  $\mathbf{p}$ , clearly cancels the first one.

### 3.3 MULTIPLE ACCESS WITHIN A CELL

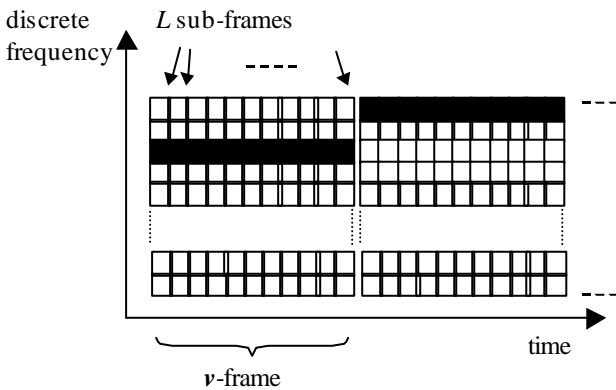


Figure 3. A multiple access scheme for R-OFDM. Each  $\mathbf{v}$ -frame has the same structure as shown in figure 2. A user occupies all  $L$  sub-frames of the same frequency index in a  $\mathbf{v}$ -frame, as indicated by the black frames. This frequency hops for different  $\mathbf{v}$ -frames to average out fading effect.

We consider the multiple access within a cell where all the users are using the same  $\mathbf{p}$ -sequence. A straightforward approach is the scheme in figure 3. The  $\mathbf{v}$ -frame for a particular user has the form

$$\mathbf{v} = \{ u_{1,k} \mathbf{x}^{(k)}, u_{2,k} \mathbf{x}^{(k)}, u_{3,k} \mathbf{x}^{(k)}, \dots, u_{L,k} \mathbf{x}^{(k)} \} \quad (12)$$

where  $\{u_{j,k}\}$  are the information symbols and  $\mathbf{x}^{(k)}$  is a length- $M$  OFDM carrier defined in (3) with frequency index  $k$ . In this way, **a user occupies all  $L$  sub-frames with frequency index  $k$  within a  $\mathbf{v}$ -frame**. It is important to keep in mind that each sub-frame  $u_{j,k} \mathbf{x}^{(k)}$  in (12) should have a prefix that is not explicitly shown only for simplicity.

Within a cell, different users are distinguished by different  $k$  values (frequency indexes). Coherent detection can be accomplished by using one sub-frame in  $\mathbf{v}$  as reference (pilot), with the rest  $L-1$  frames carrying information. This can support at most  $M$  users with orthogonal frequency separation. We can also adopt a time domain multiplexing technique with discontinuous transmission mode to support more users. For different  $\mathbf{v}$ -frames, the frequency index assigned to a user can vary (in a frequency-hopping manner) so as to average out fading effect.

In principle, the above approach is very similar to a common FDMA with frequency-hopping. Each sub-frame at a particular discrete frequency is equivalent to a modulated pulse. (A difference here is that carriers are discrete.) Consequently, R-OFDM shares many advantages of FDMA, such as intra-cell orthogonality and simple receiver complexity. However, R-OFDM has improved performance when cross-cell interference is considered, as shown below.

### 3.4 CORRELATOR TRANSCEIVER MODELS

A length- $N$  R-OFDM carrier is obtained by padding a length- $M$  OFDM carrier with appropriate zeros, define by,

$$\mathbf{z}^{(j,k)} = \{ \underbrace{0, \dots, 0}_{\text{zero frames}}, \mathbf{x}^{(k)}, \underbrace{0, \dots, 0}_{\text{zero frames}} \} \quad (13)$$

where  $\mathbf{x}^{(k)}$  is a length- $M$  OFDM carrier defined in (3). Similar to (8), the transmitter and receiver functions in figure 2 can also be expressed as,

$$\text{transmitter: } \mathbf{w} = \sum u_{j,k} \mathbf{z}^{(j,k)} \otimes \mathbf{p} \quad (14a)$$

$$\text{receiver: } \hat{u}_{j,k} = \langle \hat{\mathbf{w}}, \mathbf{p} \otimes \bar{\mathbf{z}}^{(j,k)} \rangle \quad (14b)$$

which is convenient for interference analysis. Synchronization issue

A key requirement for OFDM and R-OFDM is that all the frames should be approximately aligned. For up-link applications, the situation is more complicated since now it is necessary to consider frame alignment error among same-cell-users. Certain tolerance of alignment error can be allowed due to the use of prefixes. Such error has essentially the same effect as multi-path delay. Provided that prefix length covers the combined duration of alignment

error and multi-path delay, orthogonality among all the users can be maintained.

Generally speaking, frame alignment error is related to the round trip delay  $2r/c$ , where  $r$  is cell size and  $c$  is speed of light [10]. For example, for  $r=500$  meters,  $2r/c \approx 3.33\mu\text{s}$ . Since prefix constitutes an overhead, R-OFDM is most suitable for systems with small cell-size, such as indoor systems. For such systems, the delay spread caused by multiple reflection is also relatively small, (such as  $\sim 1\mu\text{s}$  for indoor and  $\sim 3\mu\text{s}$  for out-door systems [14]).

## 4 CROSS-CELL INTERFERENCE

In a multi-cell system, re-using the same set of carriers in different cell will cause cross-cell interference problem. R-OFDM provides a remedy to the interference problem. The basic principle is to reduce correlation among the signals from different cells. Ideally, it is preferred to minimizing peak correlation but this is generally a complicated issue [15]. A practical technique is to make interference Gaussian-noise-like. Then correlation is more evenly distributed and peak values have very small probability of occurrence. CDMA actually employs a similar principle but it is difficult to maintain intra-cell orthogonality in multi-path environments for common CDMA.

### 4.1 INTERFERENCE CHARACTERIZATION FOR THE STANDARD OFDM

We now present some detailed analysis of interference characteristics. For comparison, first consider the standard OFDM scheme in figure 1. We only discuss the transmission of one nonzero information symbol  $u$ . Results are similar if more information symbols are transmitted. From (8), the transmitted signal is  $\mathbf{v}=u\mathbf{x}$  where  $\mathbf{x}$  is an OFDM carrier defined in (3). Let  $\mathbf{v}'=u'\mathbf{x}'$  be an interfering signal. For simplicity, ignore any other channel distortions and let the received signal be  $\hat{\mathbf{v}}=u\mathbf{x}+u'\mathbf{x}'$ . Let  $u$  and  $u'$  have unit amplitude and let  $\mathbf{x}$  and  $\mathbf{x}'$  be normalized to

$$\langle \mathbf{x}, \bar{\mathbf{x}} \rangle = \langle \mathbf{x}', \bar{\mathbf{x}}' \rangle = 1$$

For the synchronous transmission, (The asynchronous case will be discussed using simulation results later.), the signal-to-interference power ratio in the decision variable  $\hat{u}$  for  $u$  is,

$$SIR = \frac{|\langle \mathbf{x}, \bar{\mathbf{x}} \rangle|^2}{|\langle \mathbf{x}', \bar{\mathbf{x}} \rangle|^2} = \frac{1}{|\langle \mathbf{x}', \bar{\mathbf{x}} \rangle|^2} \quad (15)$$

Based on the normalization assumption and Parseval's Theorem [13], the correlation power can be expressed as,

$$|\langle \mathbf{x}', \bar{\mathbf{x}} \rangle|^2 = \left| \sum_{k=0}^{N-1} \mathbf{X}'_k \bar{\mathbf{X}}_k \right|^2 = 1 \quad (16)$$

with  $\{\mathbf{X}_k\}=F(\mathbf{x})$  and  $\{\mathbf{X}'_k\}=F(\mathbf{x}')$ . For  $\mathbf{x}$  and  $\mathbf{x}'$  both defined in (3), their *DFTs* are shifted delta sequences. Consequently, the outcome of (16) is binary, i.e.,

$$|\langle \mathbf{x}', \bar{\mathbf{x}} \rangle|^2 = \begin{cases} 1 & \text{if } \mathbf{x} = \mathbf{x}' \\ 0 & \text{otherwise} \end{cases}$$

The correlation value of one implies a serious interference problem.

### 4.2 INTERFERENCE CHARACTERIZATION OF R-OFDM

For R-OFDM, let  $\mathbf{z}$  and  $\mathbf{z}'$  be from the R-OFDM carrier set defined in (13). They are convoluted by different  $\mathbf{p}$  and  $\mathbf{p}'$  respectively before transmission. With similar assumption as for the standard OFDM above,

$$SIR = \frac{1}{|\langle \mathbf{z}' \otimes \mathbf{p}', \bar{\mathbf{z}} \otimes \mathbf{p} \rangle|^2} \quad (17a)$$

Based on Parseval's Theorem [13] and (5), the correlation power in (17a) can be expressed as (with  $\mathbf{Z}=F(\mathbf{z})$ ,  $\mathbf{Z}'=F(\mathbf{z}')$ ,  $\mathbf{P}=F(\mathbf{p})$  and  $\mathbf{P}'=F(\mathbf{p}')$ )

$$|\langle \mathbf{z}' \otimes \mathbf{p}', \bar{\mathbf{z}} \otimes \mathbf{p} \rangle|^2 = \left| N \sum_{k=0}^{N-1} \mathbf{Z}'_k P'_k \bar{\mathbf{Z}}_k P_k \right|^2 \leq 1 \quad (17b)$$

From Remark 1,  $P_k P'_k = \pm 1/N$ . We assume the following two conditions.

- Sequences  $\mathbf{p}$  and  $\mathbf{p}'$  are approximately random to each other so their combined effect in (17b) is random phase shifts.
- The amplitudes of  $\{\mathbf{Z}_k\}$  and  $\{\mathbf{Z}'_k\}$  have (approximately) identical distributions.

Then using the law of large numbers, the summation in (17b) is approximately a Gaussian random variable for sufficiently large  $N$ . Large values are statistically rarer for (17b) (compared with (16) without randomization). Interference power is now more evenly distributed among carrier pairs. Such effect is referred to as interference mitigation.

### 4.3 WHEN WILL RANDOMIZATION WORK?

Condition (ii) for Gaussian assumption above may not be valid for some special cases. For example, when  $M=N$  in figure 2,  $\mathbf{z}^{(j,k)} = \mathbf{x}^{(k)}$  in (13) (i.e., no zero padding). Since an  $N$ -point *DFT* of a length- $N$   $\mathbf{x}^{(k)}$  is a delta sequence, (17b) has the same binary behavior as (16). Clearly, in this case the convolution operation by  $\mathbf{p}$  cannot provide any benefit.

On the other hand, when  $M \ll N$ , the power spectrum of an R-OFDM carrier defined in (13) is more evenly distributed. This actually introduces a spreading effect. In

particular, if  $M=1$ , every carrier  $\mathbf{z}^{(j,k)}$  in (13) contains only one non-zero symbol and its DFT spectrum has a constant amplitude over the whole frequency span of length  $N$ .

Between the two extremes, the Gaussian assumption is reasonable for (17b) for sufficiently large  $N/M$  ratio (say,  $N/M > 8$ ). We will see this more clearly in the examples below. Also notice that the relative overhead due to the use of prefix is  $D/M$  where  $D$  is the prefix length. To achieve good efficiency, we should have  $D \ll M$ . Combining the above discussion, we have the following requirement,

$$D \ll M \ll N \quad (18)$$

We conclude that to achieve effective randomization,  $\mathbf{v}$  should contain a sufficient number of sub-frames. Also notice that (18) implies that the channel delay spread (including synchronization error) should be much smaller than the channel coherent time. These conditions may restrict the application of R-OFDM to small cell-size systems.

#### 4.4 ASYNCHRONOUS INTERFERENCE

For asynchronous situations where interfering signals from other cells are not necessarily aligned, analysis is more complicated and we will only use simulation results to show the advantage of R-OFDM. Figure 4 is the histogram of pair-wise correlation power distribution, in the form of

$$|\langle \mathbf{x}', \bar{\mathbf{x}} \rangle|^2$$

for length 63 sequences. The R-OFDM sequences are generated by two different length-63  $\mathbf{p}$ -sequences according to the method discussed in Section 5. Every  $\mathbf{v}$ -frame contains 9 sub-frames of length-7 each (i.e.,  $L=9$ ,  $M=7$  and  $N=63$ ). No prefix is used for simplicity (We will discuss a more sophisticated model later). The standard OFDM sequences are generated from a 63-point *IDFT*. This length is not convenient for *FFT* implementation but it serves the purpose of comparison. The result for CDMA is also included in figure 4 for comparison, based on the correlation power between two length-63 random binary sequences.

For all the sequence pairs compared, the wanted and interfering signals have a random offset in frame alignment. The interfering signal  $\mathbf{x}'$  is constructed using two consecutive frames carrying random binary data. Notice that in this case, even two different OFDM carriers may no longer be orthogonal.

Sequences  $\mathbf{x}$  and  $\mathbf{x}'$  above can be regarded as two carriers used in neighboring cells. If they are ideal random binary sequences, their correlation power should follow an exponential distribution. The probabilities of high correlation values reduce exponentially. This can be clearly seen from the result for the random waveform CDMA in figure 4. For the standard OFDM, there is a serious correlation problem between two carriers with the

same frequency ("hit"). This is represented by the large correlation values for the standard OFDM near normalized correlation power = 1, which indicates its worst case MAI problem. For R-OFDM, correlation powers are mostly distributed in lower levels since the carriers are approximately random to each other. Overall, the correlation behavior of R-OFDM is similar to that of CDMA, although the former is somewhat irregular.

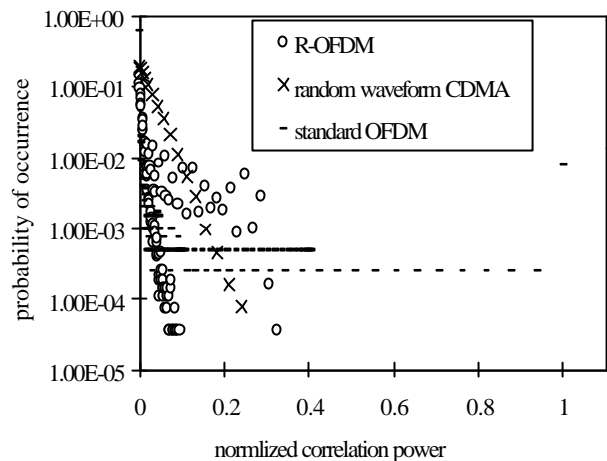


Figure 4. The distribution of correlation power for various systems with asynchronous transmission.

#### 4.5 A MORE SOPHISTICATED SYSTEM MODEL

We now introduce a more sophisticated R-OFDM system model. The parameters are:  $\mathbf{p}$  sequences length  $N = 511$  (based on length-511  $m$ -sequences), prefix length  $D = 11$ , number of sub-frames in  $\mathbf{v}$   $L = 11$  (carrying 10 information bits), sub-frame length  $M = 32$ , chip duration =  $\mu\text{s}$ , bandwidth = 1 MHz and carrier frequency = 1 GHz.

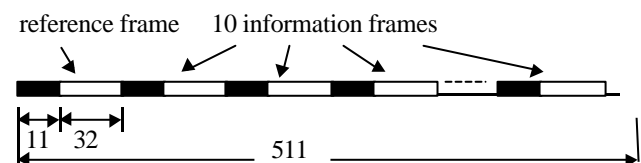


Figure 5. Structure of  $\mathbf{v}$ . A user occupies all eleven sub-frames of a unique OFDM frequency index in a  $\mathbf{v}$ -frame. The reference frame has a power level of 5dB above the signal frames. Black segments represent prefixes.

For one user, the input information is encoded by a rate  $1/2$  convolutional code (IS-95 constraint length 9 convolutional code) with 392 bits in a frame, producing a length 800 binary sequence (including 16 tailing bits), from which a length-400 complex sequence is formed in a QPSK manner. It is interleaved to generate the input information sequence (the  $\mathbf{u}$ -sequence in figure 2). A user only occupies one frequency. Thus the *IDFT* in figure 2 is actually

not necessary. We can simply modulate a complex symbol by a discrete carrier defined in (3). Each of such modulated signal form a sub-frames in  $\nu$ . Ten of such sub-frames plus a reference sub-frame are padded with respective prefixes to produce a  $\nu$ -frame in figure 5.

In fading environments, information is decodable using the phase differences between the information and the reference frames. A higher power level of the reference frame can reduce detection error. We observed that the best trade-off between system performance and transmission power is achieved by setting the reference power to about 5dB above the information frames. This is used in all the results presented below.

The length of a sub-frame together with its prefix is  $32+11=43$ . The eleven information and reference frames together with their prefixes occupy a total of 473 positions in  $\nu$ , leaving 38 positions unused. Each  $\nu$ -frame is then convoluted with a  $p$ -sequence to generate a  $w$ -frame. An extra prefix is padded at this point, see figure 2.

For convenience, we adopt the COST-207 TU (Typical Urbane) propagation models [16].

Different same-cell users are assigned with different discrete frequency indexes, see figures 3 and 4. The frequency assigned to each user changes for different  $\nu$ -frames to average out fading effect in a frequency-hopping manner.

#### 4.6 SYSTEM PERFORMANCE IN THE PRESENCE OF INTERFERENCE

We now show some experimental results about the impact of cross-cell interference. Limited by computing power, we will not deal with a full cellular system (such a 19 cell system). Instead, we will use a very simplified model, with only two cells. We will only consider up-link. The multi-path and fading effect is included but path loss is ignored first. All the signals (including interfering signals) have the same arriving power levels. It can be regarded as a worst-case interference situation<sup>4</sup>. This system model is extremely simplified, but the result can be generalized to include more cells and path loss, as discussed in 4.7.

In figure 6, we compare the interference behaviors of different systems, namely, R-OFDM, standard OFDM and CDMA. The result for the standard OFDM is obtained by removing the convolutions with  $p$ . The result for CDMA is IS-95-like, with a non-coherent four-finger rake receiver (bandwidth adjusted to 1MHz). The abscissa is normalized

<sup>4</sup> Suppose that perfect power control is used. All the same-cell user signals will have the same power level. We also assume that every user is allocated to the cell that results in minimum power transmission. Consequently, the maximum arriving power (averaged over fast fading) of an other-cell-user signal cannot exceed that of a same-cell-user signal (otherwise the former should not be assigned to its current cell).

to information rate per cell since it is not convenient to match user rate for different systems.

It is seen that error rate increases with information rate due to interference increase. For the same information rate, R-OFDM can achieve most reliable transmission. The intra-cell orthogonality of R-OFDM gives it an advantage over CDMA. The performance of standard OFDM is seriously limited by the correlation problem (the "hit" effect seen in figure 4). Notice that although orthogonal CDMA (such as the down-link of IS-95) can also achieve intra-cell orthogonality, it is difficult to maintain such orthogonality in the multi-path environments (such as the channel model used here).

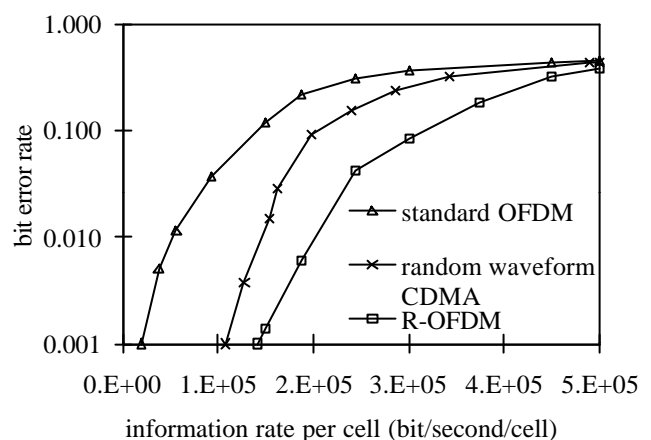


Figure 6. Simulated interference effects using a simplified two-cell model. All the signals have the same mean arriving power. Channel model: COST-207 TU (Typical Urbane) [16]. Speed = 50km/h. Chip duration = 1  $\mu$ s. Bandwidth=1 MHz. Carrier frequency =1GHz. Dual receiving antenna with equal gain combining.

#### 4.7 CAPACITY COMPARISON BETWEEN R-OFDM AND CDMA

Based on figure 6, at BER=10<sup>-3</sup>, the spectrum efficiencies for CDMA and R-OFDM are about 107 kbps/cell and 141 kbps/cell respectively.

Good performance of R-OFDM in the presence of interference shown in figure 6 implies good spectrum efficiency. Furthermore, we now show that the advantage of R-OFDM becomes more noticeable in a practical scenario (considering multi-cell and path loss), since it avoids the burden of same-cell interference. A full simulation is difficult due to computing power limitation. We will proceed employing the well-known results in [17].

A basic assumption is that average interference power determines system capacity. This assumption is widely accepted for random waveform CDMA systems (see [17]). For R-OFDM, it is approximately valid since the interference power distribution in R-OFDM is quite similar to that

in CDMA (see figure 4) without large correlation peaks for R-OFDM.

In figure 6, path loss is ignored and there are only two cells. Therefore

$$\frac{\text{total arriving same - cell - user signal power}}{\text{total arriving other - cell - user signal power}} \approx 1 \quad (19a)$$

However, according to the study in [17,18] for the up-link of a general CDMA cellular system, (assuming multi-cells, homogeneous user distribution and pass loss exponent of 4),

$$\frac{\text{total arriving same - cell - user signal power}}{\text{total arriving other - cell - user signal power}} \approx 2 \quad (19b)$$

Notice that same-cell-user interference is not affected by path loss due to power control. Thus other-cell user interference power in (19b) is only half of that in (19a). We now use this to estimate the capacity of general CDMA and R-OFDM.

For CDMA, a reduction of half of other-cell-user interference implied a factor of  $1.5/2 \approx 0.75$  for the total interference from the level in figure 6. This increases the capacity of CDMA by  $1/0.75 = 1.33$  times, i.e., from 107kbps/cell to about 143kbps/cell at  $\text{BER} = 10^{-3}$ .

For R-OFDM, a reduction of half of other-cell-user interference implied a factor of 2 for the total interference from the level in figure 6 (since there is no same-cell-user interference). This increases the capacity of R-OFDM by 2 times, i.e., from 141kbps/cell to 282kbps/cell at  $\text{BER} = 10^{-3}$ . It represents about 2 times (3dB) of capacity advantage of R-OFDM over CDMA. This clearly demonstrates the advantage of R-OFDM.

Based on the study in [17,18], eliminating same-cell MAI can lead to about 3 times (5dB) of capacity gain for CDMA. It indicates the potential for further improvement. We have observed that the fading effect has a strong impact on the single frequency carrier R-OFDM scheme in figure 3 (despite hopping on discrete frequency). Such problem can be improved by combining R-OFDM approach with other multi-carrier techniques [3-10]. This issue is still under investigation.

#### 4.8 PEAK TO AVERAGE POWER RATIO AND CLIPPING EFFECT

An inherent problem of OFDM is RF amplifier efficiency due to the multi-level modulation involved. This is also the case for R-OFDM. Clipping can be applied to the problem [19,20]. Here we consider clipping  $w = \{w_i\}$  in R-OFDM. System performance is determined by the ratio  $A^2/B^2$ , where  $A$  is the clipping amplitude and  $B^2 = E\{|w_i|^2\}$  is the mean power of the un-clipped signal (assuming unit loading resistance). Clipping may cause considerable performance degradation in a standard OFDM. However, we will demonstrate that the signal scheme in figure 3 is not

sensitive to the clipping effect. A key assumption here is that the orthogonal carriers are shared by a sufficiently large number of up-link users. We will only consider the up-link. In this case, clipping is applied individually for each user to a signal consisting of only a small subset of carriers.

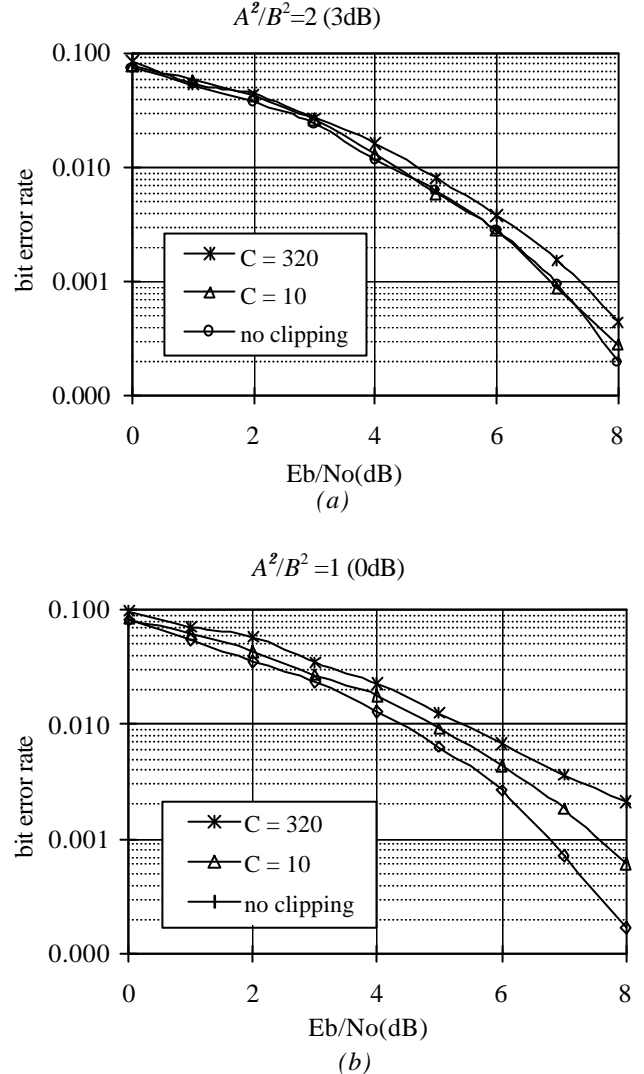


Figure 7. Clipping effect on R-OFDM in AWGN channel. No prefix is used.  $E_b$  is calculated according to the signal energy after clipping).

Let the signal obtained after clipping  $w$  be  $w + \mathbf{a}$ , where  $\mathbf{a} = \{\mathbf{a}_i\}$  is an equivalent noise sequence representing clipping error. We assume that the elements in  $w$  are Gaussian, which is reasonable due to the randomization effect  $w = v \otimes \phi$ . With this assumption, we have the mean clipping noise power,

$$E(\|\mathbf{a}\|^2) = b B^2 \quad (20a)$$

where  $b$  is a constant determined by  $A^2/B^2$ . Assume that  $w$  is normalized to  $B^2 = C/N$ , where  $C$  is the number of carri-

ers used by a user ( $C=L$  for the scheme in figure 3 but in general  $C$  can be arbitrary). Substituting this into (20a), we have

$$E(|\mathbf{a}|^2) = bC/N \quad (20b)$$

For  $N$  samples, the total clipping noise power is  $N \text{var}(\mathbf{a}) = bC$ . Assume that this noise is evenly distributed in the  $N$ -dimensional complex space  $\mathbb{Z}^N$ . The average clipping noise power per dimension is  $bC/N$ , which is also the clipping noise power affecting the decision variable of a symbol. Therefore the clipping effect is proportional to ratio  $C/N$  and its impact reduces for small  $C$ . Notice that the above analysis based on additive noise is only approximate since clipping is essential a non-linear problem.

The simulated results are shown in figure 7. When  $A^2/B^2$  is limited to 3dB, the performance loss for  $C=10$  is negligible. Even when  $A^2/B^2$  is limited to 0dB, the performance loss for  $C=10$  is only about 0.8dB at  $\text{BER}=10^{-3}$ .

Notice that the same principle applies to the standard OFDM with a small number of active subset of carriers.

Sophisticated treatments such as special coding [21] and pre-distortion [22] have been proposed to reduce peak to average power ratio. For R-OFDM, simple clipping appears sufficient for the up-link based on the discussion above.

## 5 TRANSCEIVER COMPLEXITY

This section is concerned with the design of  $\mathbf{p}$  to meet constraint (9) and efficient techniques to implement the convolution with  $\mathbf{p}$ . Let  $\mathbf{s}$  be a length- $N$   $m$ -sequence over  $\{+1, -1\}$ . It is well known [23] that  $\mathbf{s} \otimes \mathbf{s} = \{N, -1, -1, \dots, -1\}$ . Let

$$\mathbf{a} = 1/\sqrt{N+1} \text{ and } \mathbf{b} = (1 \pm \sqrt{N+1})/N \quad (21)$$

and  $\mathbf{e}$  be an all-1 sequence. Then it can be verified that  $\mathbf{p} = \mathbf{a}\mathbf{s} + \mathbf{b}\mathbf{e}$  satisfies (9) [23]. For such  $\mathbf{p}$ ,  $\mathbf{v} \otimes \mathbf{p}$  can be implemented as the follows. Since  $\mathbf{v} \otimes \mathbf{p} = \mathbf{a}\mathbf{v} \otimes \mathbf{s} + \mathbf{b}\mathbf{v} \otimes \mathbf{e}$  and  $\mathbf{v} \otimes \mathbf{e}$  is trivial, we only need to concentrate on  $\mathbf{v} \otimes \mathbf{s}$ . In matrix form,

$$\mathbf{v} \otimes \mathbf{s} = \begin{bmatrix} v_0 & \dots & v_{N-1} \end{bmatrix} \begin{bmatrix} s_0 & s_1 & \dots & s_{N-1} \\ s_{N-1} & s_0 & \ddots & \\ & \ddots & \ddots & s_1 \\ s_1 & \dots & s_{N-1} & s_0 \end{bmatrix} = \mathbf{v}\mathbf{S} \quad (22)$$

The columns of  $\mathbf{S}$  are the cyclic shifts of a length- $N$   $m$ -sequence. Augment  $\mathbf{S}$  by an all-1 row and an all-1 column to

$$\mathbf{P} = \begin{pmatrix} \mathbf{1} & \mathbf{I} \\ \mathbf{I} & \mathbf{S} \end{pmatrix} \quad (23)$$

Then

$$[\mathbf{v} \otimes \mathbf{e}, \mathbf{v} \otimes \mathbf{s}] = [\mathbf{0}, \mathbf{v}]\mathbf{P} \quad (24)$$

Let  $N'=N+1$ . It can be shown (Appendix) that there exist permutation matrixes  $\mathbf{A}$  and  $\mathbf{B}$  such that  $\mathbf{P} = \mathbf{A}\mathbf{H}\mathbf{B}$ , where  $\mathbf{H}$  is a  $N' \times N'$  Hadamard matrix, i.e.,

$$[\mathbf{v} \otimes \mathbf{e} \quad \mathbf{v} \otimes \mathbf{s}] = [\mathbf{0} \quad \mathbf{v}]\mathbf{A}\mathbf{H}\mathbf{B} \quad (25)$$

Different  $m$ -sequences result from different selection of the permutation matrixes  $\mathbf{A}$  and  $\mathbf{B}$ . Such  $m$ -sequences are approximately random to each other. The corresponding transmitter and receiver structures are shown in figure 8, where  $F^{-1}$  and  $F$  can be realized by *FFT* (Fast Fourier Transforms). At the transmitter, an *FFT* if not be necessary if a user may only occupy a few carriers. At the receiver, a full DFT is necessary to separate all the users so an *FFT* can bring cost down. The multiplication by  $\mathbf{H}$  can be implemented by an *FHT* (Fast Hadamard Transform). Both *FFT* and *FHT* are well known for their efficiency (an *FHT* costs only  $N' \log_2 N'$  additions). The complexity involved in figure 8 is only marginally higher than an ordinary OFDM transmitter and receiver pair.

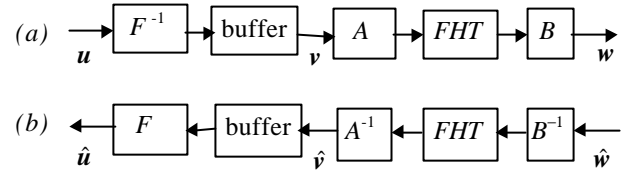


Figure 8. Transceiver structure for R-OFDM: (a) transmitter and (b) receiver. Blocks labeled by  $A, A^{-1}, B$  and  $B^{-1}$  are interleavings related to  $A$  and  $B$  defined in (23). The buffers are used to handle the sub-frames in a  $\mathbf{v}$ -frame. In this structure, different same-cell-users are separated by the discrete frequencies. Different other-cell-users are separated by different interleaving  $A$ - $B$  pairs.

## 6 CONCLUSIONS

In this paper, we have demonstrated a number of advantages for R-OFDM. The followings can be drawn from the analytical and simulation studies presented above.

- R-OFDM can achieve intra-cell orthogonality and cross-cell MAI mitigation simultaneously in multipath environments.
- Provided that a sufficient number of sub-frames are involved, convolutional scrambling can achieve good randomization effect.
- When a user only occupies a small subset of carriers and clipping is individually applied for each user, R-OFDM is not sensitive to the clipping effect. This implies relaxed requirement on RF amplifier.
- R-OFDM transmitter and receiver can be implemented with relatively low complexity.

## APPENDIX. TRANSFORMATION BETWEEN M-SEQUENCES AND HADAMARD SEQUENCES

In the following we will discuss binary codes over GF[2]. The required  $m$ -sequences discussed in section VI can be obtained using the standard mapping

$$\{0 \rightarrow -1, 1 \rightarrow 1\} \quad (26)$$

A  $2^m$ -th order Hadamard matrix  $H$  in GF[2] is defined by its  $(i, j)$ -th entry as [17]

$$H_{i,j} = \left( \sum_{k=0}^{m-1} i_k j_k \right) \bmod 2 \quad (27)$$

where  $i_k$  and  $j_k$  are the  $k$ th bit of the binary expression of  $i$  and  $j$  respectively, i.e.,

$$i = \sum_k i_k 2^k \quad \text{and} \quad j = \sum_k j_k 2^k \quad (28)$$

Every row of the following matrix is a length  $2^m-1$   $m$ -sequence (also called maximum length code [24]) augmented with a zero at the front,

$$P = \begin{pmatrix} 0 & 0 & 0 & \dots & 0 \\ 0 & \text{tr}(\mathbf{a}^0) & \text{tr}(\mathbf{a}^1) & \dots & \text{tr}(\mathbf{a}^{2^m-2}) \\ 0 & \text{tr}(\mathbf{a}^{2^m-1}) & \text{tr}(\mathbf{a}^0) & \dots & \text{tr}(\mathbf{a}^{2^m-3}) \\ \vdots & \vdots & \vdots & \vdots & \vdots \\ 0 & \text{tr}(\mathbf{a}^1) & \text{tr}(\mathbf{a}^2) & \dots & \text{tr}(\mathbf{a}^0) \end{pmatrix} \quad (29)$$

or

$$P_{i,j} = \begin{cases} \text{tr}(\mathbf{a}^{j-i}) & \text{for } ij \neq 0 \\ 0 & \text{for } ij = 0 \end{cases} \quad (30)$$

where  $\mathbf{a}$  is a primitive root in GF[ $2^m$ ] and  $\text{tr}(\mathbf{a}^i)$  is the trace of  $\mathbf{a}^i$ . Clearly, ignore the first column,  $P$  are formed by all the cyclic-shifts of an  $m$ -sequence (It is the mapping on GF(2) of the matrix in (22) bearing the same name). Our aim below is to find row and column permutations (the interleaving schemes in figure (8) which transform  $H$  into  $P$ ).

Any element  $\mathbf{a}^i$  of GF[ $2^m$ ] can be expressed as,

$$\mathbf{a}^i = \sum_{k=0}^{m-1} b_{i,k} \mathbf{a}^k \quad (31)$$

where  $b_{i,k} \in \text{GF}[2]$ . Based on this we define an one to one mapping  $\mathbf{f}(i)$  from  $(0, 1, \dots, 2^m-2)$  to  $(1, \dots, 2^m-1)$

$$\mathbf{f}(i) = \sum_{k=0}^{m-1} b_{i,k} 2^k \quad i \neq 0 \quad (32)$$

where  $b_{i,k}$  is used as an ordinary integer. From (27) and (31),

$$\mathbf{a}^{-\mathbf{f}^{-1}(i)} = \sum_{k=0}^{m-1} i_k \mathbf{a}^k \quad (33)$$

Define another one to one mapping  $\mathbf{g}(j)$  from  $(0, 1, \dots, 2^m-2)$  to  $(1, \dots, 2^m-1)$ ,

$$\mathbf{g}(j) = \sum_{k=0}^{m-1} \text{tr}(\mathbf{a}^{j+k}) 2^k \quad (34)$$

so that,

$$\text{tr}(\mathbf{a}^{y^{-1}(j)+k}) = j_k \quad \text{for } j \neq 0 \quad (35)$$

From (29), for  $ij \neq 0$

$$\begin{aligned} P_{\mathbf{f}^{-1}(i)+1, \mathbf{g}^{-1}(j)+1} &= \text{tr}(\mathbf{a}^{\mathbf{g}^{-1}(j)-\mathbf{f}^{-1}(i)}) \\ &= \text{tr}\left(\sum_{k=0}^{m-1} i_k \mathbf{a}^{\mathbf{g}^{-1}(j)+k}\right) \quad \text{using (33)} \\ &= \sum_{k=0}^{m-1} i_k \text{tr}(\mathbf{a}^{\mathbf{g}^{-1}(j)+k}) \\ &= \sum_{k=0}^{m-1} i_k j_k = H_{i,j} \quad \text{using (35)} \end{aligned}$$

Therefore the required permutations are

$$\begin{aligned} \text{Row permutation: } & 0 \oplus 0 \\ & i \rightarrow \mathbf{f}^{-1}(i)+1 \quad \text{for } i \neq 0 \\ \text{Column permutation: } & 0 \oplus 0 \\ & j \oplus \mathbf{g}^{-1}(j)+1 \quad \text{for } j \neq 0 \end{aligned}$$

Finally, different selections of the primitive element  $\alpha$  result in different  $m$ -sequences in (29) as well as different mappings defined in (32) and (34). In practice, it is more efficient to interleave a reference  $m$ -sequence to obtain all the  $m$ -sequences, see [15] for details.

## ACKNOWLEDGEMENT

The author wishes to thank J.L. Zhang for his valuable help in this work.

*Manuscript received on ...*

## REFERENCES

- [1] M. Alard and R. Lassalle. Principle of modulation and channel coding for digital broadcasting for mobile receivers. *EBU Review*, No. 224, pages 168-190, August 1987.
- [2] B. L. Floch, M. Alard and C. Berrou. Coded orthogonal frequency division multiplex. *Proc. IEEE*, Vol. 83. No. 6, pages 982-996, June 1995.
- [3] S. Kaiser and K. Fazel, *Multi-Carrier Spread-Spectrum & related Topics*. Kluwer Academic Publications, 1999.
- [4] K. Fazel. Performance of CDMA-OFDM for mobile communications In *Proc. IEEE. Int. Conference on Universal Personal Communications*, pages 975-979, OCT 1993.

- [5] S. Kaiser. OFDM-CDMA versus DS-CDMA; performance evaluation for fading channels. In *Proc IEEE ICC'95*, Seattle, pages 1722-1725, June 1995.
- [6] H. Sari, F. Vanhaverbeke and M. Moeneclaey. Some novel concepts in multiplexing and multiple access, in *Multi-Carrier Spread-Spectrum & related Topics*. pages 3-12, Kluwer Academic Publications 1999.
- [7] N. Yee, J-P. Linnarz and G. Fettweis. Multi-carrier CDMA in indoor wireless radio network. *IEICE Trans. Commun.*, Vol. E77-B, pages 900-904, July 1994.
- [8] L. Tomba and W.A. Krzymien. Downlink detection scheme for MC-CDMA systems in indoor environments, *IEICE Trans. Commun.*, Vol. E79-B, pages 1351-1360, Sept. 1996.
- [9] S. Hara and R. Prasad, Overview of multi-carrier CDMA, *IEEE Communications Magazine*, Vol. 35, No. 12, pages 126-133, Dec. 1997.
- [10] S. Kaiser and W.A. Krzymien. Performance effects of the uplink asynchronism in a spread spectrum multi-carrier multiple access system. *European Transaction on Communications*, Vol. 10, No. 4, July-Aug. 1999.
- [11] Li Ping. A Combined OFDM-CsDMA Approach to Cellular Mobile Communications. *IEEE Trans. Communications*, Vol. 47, No. 7, pages 979-982, July 1999.
- [12] S. Moshavi. Multi-user detection for DS-CDMA communications. *IEEE Communication Magazine*, Vol. 34, No. 10, pages 124-136, Oct. 1996.
- [13] J.G. Proakis and D. G. Manolakis. *Digital Signal Processing*. Maxwell Macmillan International, 1992.
- [14] T. S. Rappaport. *Wireless Communications; Principle and Practice*. Prentice Hall, 1996.
- [15] D.V. Sarwate and M.B. Pursley. Cross correlation properties of pseudo-random and related sequences. *Proc. IEEE*, Vol. 68, No.5, pp. 593-619, May 1980.
- [16] ETSI/TC GSM Recommendation 05.05.
- [17] K.S. Gilhousen, I.M. Jacobs, R. Padovani, A.J. Viterbi, L.A. Weaver and Jr., C.E. Wheatly. On the capacity of a cellular CDMA system. *IEEE Trans. Vehicular Technol.* Vol. 40, No. 2, pages 303-312, May 1991.
- [18] A. Viterbi. The orthogonal-random waveform dichotomy for digital mobile personal communication. *IEEE Personal Communications Magazine*, pages 18-24, No. 1, 1994.
- [19] J. Rinne and M. Renfors. The behavior of orthogonal frequency division multiplexing signals in an amplitude limiting channel. In *Proc. IEEE ICC'94*, pages 381-385, May 1995.
- [20] X. Li and L.J. Cimini, Jr. Effects of clipping and filtering on the performance of OFDM. *IEEE Communications Letters*, Vol. 2, No. 5, pages 131-133, May 1998.
- [21] A.J. Grant and R. van Nee. Efficient maximum likelihood decoding of peak power limiting for OFDM. In *Proc. IEEE Vehicular Technology Conference*, pages 2081-2084, 1998.
- [22] P. Banelli and S. Cacopardi. Theoretical analysis and performance of OFDM signals in nonlinear AWGN channels. *IEEE Transactions on Communications*, Vol. 48, No. 3, pages 430-441, March 2000.
- [23] H. Haroshi, G. Wu, K. Taira, Y. Hase and H. Sasaoka. A new multi-code high speed mobile radio transmission scheme using cyclic modified m-sequence. In *Proc. IEEE Vehicle Technology Conference*, pages 1709-1713, May 1997.
- [24] F.M. MacWilliams and N.j.A. Sloane. *The Theory of Error-Correcting Codes*. North-Holland, Amsterdam, 1977.